Nonlinear oscillators for vibration energy harvesting

L. Gammaitoni,[a] I. Neri, and H. Vocca
Dipartimento di Fisica, NiPS Laboratory, Università di Perugia, I-06123 Perugia, Italy, and Istituto Nazionale di Fisica Nucleare, Sezione di Perugia, I-06123 Perugia, Italy

(Received 11 March 2009; accepted 23 March 2009; published online 22 April 2009)

Vibration to electricity energy conversion strategies are discussed by using nonlinear stochastic dynamics. General principles for the exploitation of nonlinear oscillators in energy harvesting that provide useful leads for the realization of micropower generators of practical interest are presented. © *2009 American Institute of Physics*. [DOI: 10.1063/1.3120279]

The search for solutions in powering small portable electronic devices has been, in recent years, the subject of a relevant scientific and technological effort worldwide.[1,2] The powering of remotely distributed wireless microsensors is a very challenging task due to the fact that the traditional approach based on batteries revealed impracticable for a number of reasons, chief among them is the impossibility to replace them once they have exhausted their charge. On the other hand, especially in the case of mobile devices, it is highly desirable to have power sources colocated with the microdevices. The current solution is to harvest the ambient energy where and when necessary, whether this be electromagnetic (light), thermal, or mechanical in nature. Due to the almost ubiquitous presence of ambient kinetic energy, mostly in the form of random vibrations, a significant attention has been devoted to the conversion of mechanical energy into electric power exploiting piezoelectricity,[3] electromagnetic induction or capacitance variations.[4,5] In all these cases, the traditional approach is based on the resonant tuning of the mechanical oscillator. However, difficulties arise both because the tuning of the oscillators is constrained by geometrical factors and because the energy spectra of the available vibration are commonly spread in a wide frequency range, with the prevalence of low frequency components.

In a recent paper,[6] it has been proposed to overcome such limitations by considering non-linear oscillators instead of linear, i.e., resonant, ones. Specifically, it has been shown that a bistable oscillator (a biased inverted pendulum) can outperform a linear oscillator (simple inverted pendulum) in the presence of a wide spectrum vibration if some bias parameter is optimized.

In this letter we show that the results presented in Ref. 6 represent a special case of a more general behavior and that the increased performances of nonlinear oscillators can be found, also in monostable/multistable nonlinear dynamics achievable in a number of different systems and geometries. For the sake of concreteness we will focus on the functioning of a piezoelectric energy harvesting device,[3] though most of the considerations presented here are applicable also to other energy conversion mechanisms based on dynamical oscillators. Strain in a piezoelectric material causes charge separation and produces an electric field and consequently a voltage drop V proportional to the stress applied. The piezoelectric oscillator is usually realized with a cantilever beam structure with a mass at one end of the lever and is acted on by the vibration applied to the other end. The voltage produced varies with the strain that is a function of the applied vibrations.

Let us consider a generic piezoelectric oscillator, whose dynamics can be represented by the following system of coupled equations:[6,7]

$$\ddot{x} = -\frac{dU(x)}{dx} - \gamma\dot{x} - K_v V + \sigma\xi(t), \tag{1}$$

$$\dot{V} = K_c\dot{x} - \frac{1}{\tau_p}V, \tag{2}$$

where x represents the relevant observable of the oscillator dynamics and V is the value of the voltage drop. $U(x)$ is the potential energy function, γ is the viscous friction coefficient, and K_v is the coupling coefficient that relates the oscillation to the voltage. The effect of the vibration is mimicked by the random force $\sigma\xi(t)$ (a stochastic process with Gaussian distribution, zero mean, and unitary standard deviation, and exponential autocorrelation function with correlation time τ). K_c is the coupling constant of the piezoelectric sample. The time constant of the piezoelectric dynamics τ_p is related to the coupling capacitance C and to the resistive load R by $\tau_p = RC$. We start our analysis by considering a quartic bistable potential:[6]

$$U(x) = -\tfrac{1}{2}ax^2 + \tfrac{1}{4}bx^4. \tag{3}$$

The potential function $U(x)$ is symmetric and bistable when $a>0$ and monostable for $a\leq 0$. In the bistable case, the two minima at $\pm x_m = \pm\sqrt{a/b}$ are separated by a barrier whose maximum is at $x=0$ and whose height is $\Delta U = U(0) - U(x_m) = a^2/4b$. We are interested in computing $V(t)$, the voltage drop across the load resistance R by the moment that the power attainable[8] at the system output is V^2/R. In Fig. 1 we present a 3D plot of the averaged root-mean-square voltage $V_{\rm rms} = \sqrt{\langle V^2\rangle - \langle V\rangle^2}$ as a function of the two parameters a and b obtained via a digital solution of the stochastic differential equations in (1) and (2). For a fixed value of b, the $V_{\rm rms}$ shows a pronounced maximum as a function of a, located in the $a>0$ region, i.e. in the strongly nonlinear (bistable) region.[6] Quite remarkably, if we fix a, the $V_{\rm rms}$ shows a maximum, as a function of b also, only if $a>0$. Two conditions have to be met in order to have a maximum in the $V_{\rm rms}$: (i) the $x_{\rm rms}$ has to be as large as possible, and; (ii) the $x_{\rm rms}$ amplitude has to be transduced into $V_{\rm rms}$ with minor losses and this can happen if $V(t)$ can follow closely the

[a]Electronic mail: luca.gammaitoni@pg.infn.it.

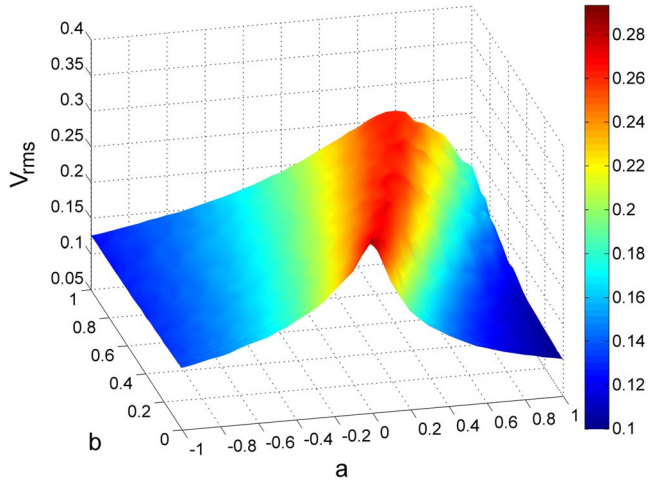

FIG. 1. (Color online) 3D plot of $V_{\rm rms}$ vs a and b for the Duffing potential case. Here $\gamma=0.5$, $\sigma=0.6$, $\tau=10$, $\tau_p=10^4$, $K_c=0.5$, and $K_v=0.5$.

evolution of $x(t)$. Clearly, the condition (ii) is constrained by the form of Eq. (2) that acts as a high-pass filter for $x(t)$, with cut-on frequency determined by $\omega_p=1/\tau_p$.

In Fig. 2 we show $K_v x_{\rm rms}$ and $V_{\rm rms}$ as a function of a for a fixed value of b and for different values of ω_p. As it is well evident on decreasing ω_p, the two curves for $K_v x_{\rm rms}$ and $V_{\rm rms}$ became closer and closer. In the limit $\omega_p \to 0^+$, i.e., $\tau_p \to \infty$, $V_{\rm rms}=K_v x_{\rm rms}$ as predicted by Eq. (2). Due to the high-pass filter effect of Eq. (2), in order to have most of the motion $x(t)$ transduced into the voltage $V(t)$ it is important that most of the energy in $x(t)$ is located at frequencies larger than ω_p. By the moment that the voltage V (and thus the power), peaks for $a>0$ we focus our attention on the bistable region.

The dynamic of $x(t)$ in this region is characterized by a complex motion composed mainly by oscillations around each of the two minima $\pm x_m$ (intrawell dynamics) plus random crossings over the potential barrier (interwell dynamics).[9] The intrawell dynamics consists of localized oscillations characterized by frequencies close to $U''(x_m)=2a$ and relatively small amplitudes. On the other hand, the interwell dynamics is characterized by a relatively large amplitude (of the order of $2x_m$) and consists of random crossings

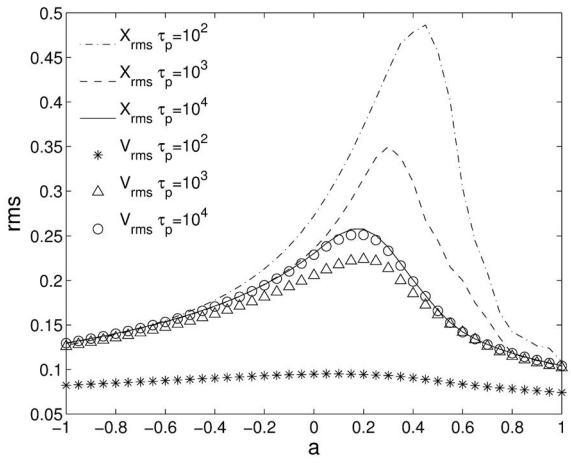

FIG. 2. $V_{\rm rms}$ (symbols) and $K_v x_{\rm rms}$ (lines) vs a for the Duffing potential case. Here $b=0.3$ and $\sigma=0.3$. The other parameters value are as in Fig. 1.

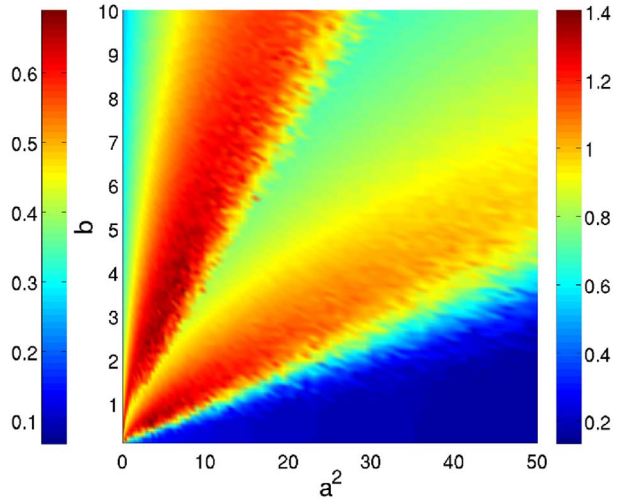

FIG. 3. (Color online) $V_{\rm rms}$ vs a^2 and b. Two different plots for the Duffing potential case are superimposed on the same graph. The plot on the leftmost side of the figure (color grade scale left) refers to the case of $D=0.09\times 10$, while the plot on the right (color grade scale right) refers to the case of $D=0.36\times 10$. The other parameters value are as in Fig. 1.

whose average rate, the so-called Kramers rate,[10,11] can be expressed as a function of both the noise intensity and the barrier height ΔU and is proportional to $\exp(-\Delta U/D)$. Here $D=\sigma^2\tau$ represents the noise intensity. For a wide range of parameter values, the crossings dynamics is the slowest dynamics in the system. In order to obtain a large V it is required that, given a certain noise intensity, the ΔU has to satisfy the condition $k\exp(-\Delta U/D)\geq\omega_p$, where k is a constant of the order of unity, i.e.,

$$b \geq \frac{a^2}{4D\log\tau_p}. \tag{4}$$

On the other hand, from the (i) condition we can easily see that a maximum in $x_{\rm rms}$ requires that x_m is as large as possible. Putting together these two conditions we obtain

$$b_M = \frac{a^2}{4D\log\tau_p}. \tag{5}$$

In Fig. 3 we show two superimposed pseudocolor plots of $V_{\rm rms}$ for two different values of the noise intensity D. As it is apparent the position of the maxima in the a^2-b plane develops along an approximately straight line, in agreement with Eq. (5). Moreover, we notice that the amplitude of the $V_{\rm rms}$ maxima decreases when a increases. This can be easily accounted for by noticing that such a maximum is clearly proportional to the maximum of $x_m=\sqrt{a/b_M}$ and thus, using Eq. (5), it decreases as $\sqrt{1/a}$.[12]

Based on the simple leads from the Duffing case, it is immediate now to inquire if the bistability condition that we have considered is a necessary condition or not. In order to keep things simple we focused on the following form, $U(x)=ax^{2n}$, with $a>0$ and $n=1,2,\ldots$. For $n=1$ we have the linear potential with resonant dynamics, usually employed in standard harvesting strategies, while for $n>1$ we are in the nonlinear, monostable case.

In Fig. 4 we show the $x_{\rm rms}$ as a function of a and n. For the sake of simplicity we considered the case where τ_p is large enough so that $V_{\rm rms}\approx K_v x_{\rm rms}$ and the main result can be applied to $V_{\rm rms}$ as well.

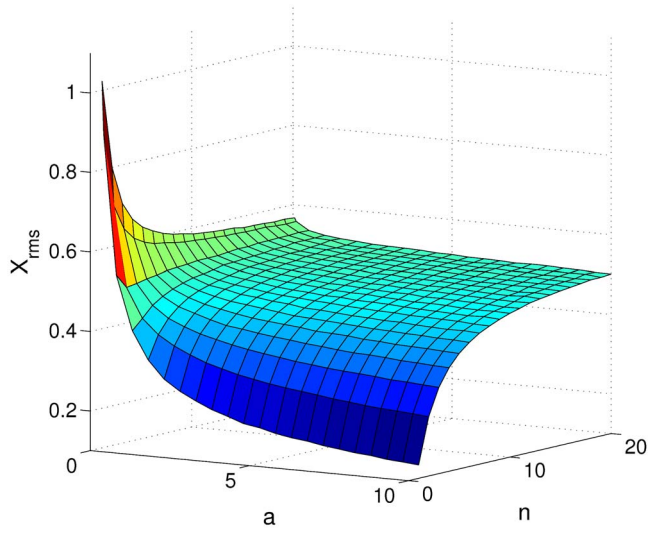

FIG. 4. (Color online) 3D plot of x_{rms} vs a and n for the ax^{2n} potential case. $\sigma=0.6$, $\tau_p=10^4$, and $\tau=10$.

Quite remarkably, if a is larger than a certain a_{th} then x_{rms} increases with n and a nonlinear potential can easily outperform a linear one, thus extending the main finding of the Duffing case also to the monostable case. On the other hand if $a<a_{th}$ then x_{rms} decreases with n and the linear case performs better than the nonlinear case. The value of a_{th} can be determined by the following argument. It can be shown that

$$x_{rms}^2=\frac{\int_{-\infty}^{+\infty}x^2e^{-ax^{2n}/D}dx}{\int_{-\infty}^{+\infty}e^{-ax^{2n}/D}dx}. \tag{6}$$

x_{rms} appears to be a decreasing function of n when $a \leq D/4f(n)$ and an increasing function of n when $a>D/4f(n)$, where $f(n)$ is a slowly varying function of n that can be approximated to unity. This suggests the value for the $a_{th}\approx D/4=\sigma^2\tau/4$ in fairly good agreement with the results presented in Fig. 4. In a real world application, in a device designed for energy harvesting, the value of the noise intensity D is set by the ambient. The value of the parameter a is usually set by the dynamical constraints or by the material properties (stiffness, inertia, etc.), while the value of n can sometimes be selected by a proper design of the geometry of the device, thus potentially improving the device performances.

In conclusion we have demonstrated that the nonlinear dynamical properties of a noise activated energy harvesting device can play a favorable role in enhancing the performances in terms of power produced (proportional to V_{rms}^2). Moreover we have shown that such an advantage is not a peculiar property of bistable systems[6] but can be extended to nonlinear monostable systems as well, provided that some care is taken in selecting the proper nonlinear dynamical properties.

The authors gratefully acknowledge financial support from Ministero Italiano della Ricerca Scientifica (PRIN 2007) and European Commission (FPVI, STREP, Contract No. 034236, SUBTLE: Sub KT Low Energy Transistors and Sensors).

[1] J. A. Paradiso and T. Starner, IEEE Pervasive Comput. **4**, 18 (2005).
[2] S. Roundy, P. K. Wright, and J. M. Rabaey, *Energy Scavenging for Wireless Sensor Networks* (Kluwer, Dordrecht, 2003).
[3] S. R. Anton, and H. A. Sodano, Smart Mater. Struct. **16**, R1 (2007).
[4] S. Meninger, J.-O. Mur-Miranda, R. Amirtharajah, A. Chandrakasan, and J. Lang, IEEE Trans. Very Large Scale Integr. (VLSI) Syst. **9**, 64 (2001).
[5] P. D. Mitcheson, T. C. Green, E. M. Yeatman, and A. S. Holmes, J. Microelectromech. Syst. **13**, 429 (2004).
[6] F. Cottone, H. Vocca, and L. Gammaitoni, Phys. Rev. Lett. **102**, 080601 (2009).
[7] E. Lefeuvre, A. Badel, C. Richard, L. Petit, and D. Guyomar, Sens. Actuators, A **126**, 405 (2006).
[8] Y. C. Shu and I. C. Lien, Smart Mater. Struct. **15**, 1499 (2006).
[9] L. Alfonsi, L. Gammaitoni, S. Santucci, and A. R. Bulsara, Phys. Rev. E **62**, 299 (2000).
[10] H. Kramers, Physica (Utrecht) **7**, 284 (1940).
[11] P. Hänggi, P. Talkner, and M. Borkovec, Rev. Mod. Phys. **62**, 251 (1990).
[12] L. Gammaitoni, 2009 (unpublished).